

# Lower-Critical Dimension of the Random-Field XY Model and the Zero-Temperature Critical Line

Kutay Akin<sup>1,2</sup> and A. Nihat Berker<sup>3,4,5</sup>

<sup>1</sup>*Department of Electrical and Electronics Engineering, Boğaziçi University, Bebek, Istanbul 34342, Turkey*

<sup>2</sup>*Department of Physics, Boğaziçi University, Bebek, Istanbul 34342, Turkey*

<sup>3</sup>*Faculty of Engineering and Natural Sciences, Kadir Has University, Cibali, Istanbul 34083, Turkey*

<sup>4</sup>*TÜBİTAK Research Institute for Fundamental Sciences, Gebze, Kocaeli 41470, Turkey*

<sup>5</sup>*Department of Physics, Massachusetts Institute of Technology, Cambridge, Massachusetts 02139, USA*

The random-field XY model is studied in spatial dimensions  $d = 3$  and 4, and in-between, as the limit  $q \rightarrow \infty$  of the  $q$ -state clock models, by the exact renormalization-group solution of the hierarchical lattice or, equivalently, the Migdal-Kadanoff approximation to the hypercubic lattices. The lower-critical dimension is determined between  $3.81 < d_c < 4$ . When the random-field is scaled with  $q$ , a line segment of zero-temperature criticality is found in  $d = 3$ . When the random-field is scaled with  $q^2$ , a universal phase diagram is found at intermediate temperatures in  $d = 3$ .

## I. INTRODUCTION: ISING AND XY LOWER-CRITICAL DIMENSIONS

Quenched randomness strongly affects the occurrence of order at low spatial dimension  $d$ , reflected as the lower-critical dimension  $d_c$  below which no ordering occurs for a given class of systems. In the random-magnetic-field  $n = 1$  component spin Ising model, after a strong experimental and theoretical controversy between  $d_c = 2$  claims [1–3] and  $d_c = 3$  claims [4], the issue was settled for  $d_c = 2$ . [5, 6] The fact that  $d_c$  is not 3 fell in contradiction with the prediction of a dimensional shift of 2 due to random fields coming from all-order field-theoretic expansions from  $d = 6$  down to  $d = 1$  [7], which indeed is a considerable distance to expand upon for a small-parameter expansion of  $\epsilon = 6 - d$ . In this study, the logically next model, namely the  $n = 2$  components spin XY model under random fields is examined and surprising results are obtained, this time in near-agreement with the dimensional shift of 2, but also with an interesting zero-temperature critical line segment and a universal scaled finite-temperature phase diagram.

Random-field Ising results supporting  $d_c = 2$  were obtained [5, 6] by the Migdal-Kadanoff [8, 9] renormalization-group calculations in  $d = 2$  (no random-field order),  $d = 2.32$  (random-field order), and  $d = 3$  (more random-field order). In the same vein, for the random-field XY model, Migdal-Kadanoff renormalization-group calculations are done here in  $d = 3$  and 4, and in between. The Migdal-Kadanoff renormalization-group calculation (Fig. 1) is a highly successful, flexible, and therefore most used today and today, physically motivated approximation for hypercubic lattices and, simultaneously, an exact calculation for  $d$ -dimensional hierarchical lattices [10–12]. The hierarchical lattice connection makes the Migdal-Kadanoff procedure a physically realizable approximation. For recent work using hierarchical lattices, see Refs. [14–21]. Migdal-Kadanoff-hierarchical-lattices correctly give the lower-critical dimensions of  $d_c = 1$  of the Ising

model [8, 9],  $d_c = 2$  of the XY [22, 23] and ( $n = 3$  spin components) Heisenberg [24] models in the absence of quenched randomness. For the much more complex system with competing quenched-random interactions, Migdal-Kadanoff gives the non-integer  $d_c = 2.46$  for the Ising spin-glass system. [25–31] In addition to giving the lower-critical temperatures, it yields such diverse results as, e.g., the low-temperature algebraic order of the  $d = 2$  XY model [22, 23], the chaotic nature [32–34] of the ferromagnetic-antiferromagnetic [35] and left-right chiral [36] Ising spin glasses, and the changeover from second- to first-order phase transitions of  $q$ -state Potts models in  $d = 2$  and 3. [37]

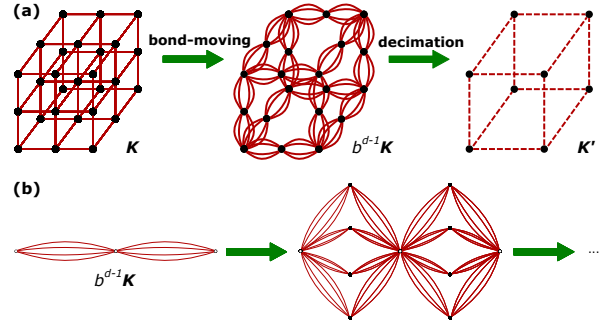


FIG. 1. From Ref.[38]: (a) Migdal-Kadanoff approximate renormalization-group transformation for the  $d = 3$  cubic lattice with the length-rescaling factor of  $b = 2$ . (b) Construction of the  $d = 3, b = 2$  hierarchical lattice for which the Migdal-Kadanoff recursion relation is exact. For general spatial dimension  $d$ , the bond-moving is  $(b^{d-1})$ -fold. The renormalization-group solution of a hierarchical lattice proceeds in the opposite direction of its construction.

## II. MODEL AND METHOD

The XY model is approached as the  $q \rightarrow \infty$  limit of the  $q$ -state clock models. In the  $q$ -state clock models, at each site  $i$  of the lattice, a planar unit spin  $\vec{s}_i$  can

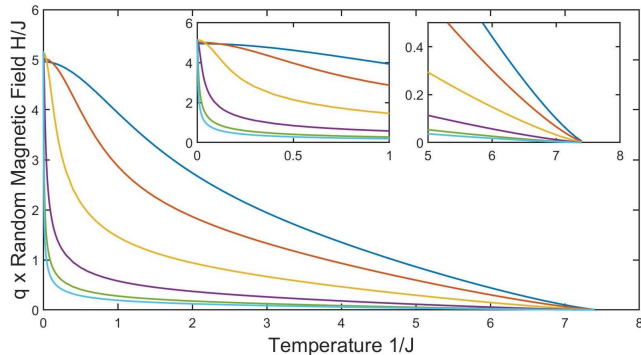


FIG. 2. Phase diagrams for  $(q = 7, 10, 20, 50, 100, 150)$ -state random-field clock models in  $d = 3$ , occurring in the figure respectively from high field to low field. Disordered and ferromagnetic phases occur at high temperature-high field and low temperature-low field, respectively. It is seen that the ferromagnetic phase, in random field, disappears as  $q \rightarrow \infty$ , indicating that no ferromagnetic phase occurs in the random-field XY model at non-zero temperature in  $d = 3$ . However, for high  $q$ , the ordered phase extends to  $qH/J = 5.1$  at zero temperature, as also seen in the left box. For high  $q$ , the zero-field ferromagnetic transition temperature saturates, as also seen in Ref.[38] and in the left box in this figure.

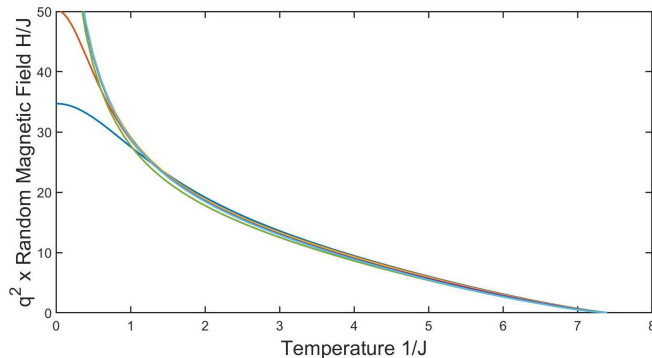


FIG. 3. Phase diagrams for  $(q = 7, 10, 20, 50, 100, 150)$ -state random-field clock models in  $d = 3$ . At low temperature, the curves are, from low field to high field,  $q = 7, 10$  and indistinguishably  $q = 20, 50, 100, 150$ . It is seen that, when the random field is scaled with  $q^2$ , a universal phase diagram is found above low temperature for high  $q$ .

point in one of  $q$  directions in the plane, namely with the angle  $\theta_k = k(2\pi/q)$ , where  $k = 0, 1, \dots, q - 1$ . A detailed renormalization-group study on the phase transitions and thermodynamics of the  $q$ -state clock models, without quenched randomness, has been done.[38] The currently studied  $q$ -state clock model, with quenched random fields, is defined by the Hamiltonian

$$-\beta\mathcal{H} = \sum_{\langle ij \rangle} (J\vec{s}_i \cdot \vec{s}_j + \vec{s}_i \cdot \vec{H}_i + \vec{s}_j \cdot \vec{H}_j), \quad (1)$$

where  $\beta = 1/k_B T$  and sum is over all nearest-neighbor pairs of spins. In each term in the sum, the random-fields

$\vec{H}_i, \vec{H}_j$  have magnitude  $H$  and each randomly points along one of the allowed directions  $\theta_k$ .

We solve this model using the Migdal-Kadanoff renormalization group. The local renormalization-group transformation is given in Fig. 1 and is simple to implement in systems without quenched randomness. With our currently studied quenched random-field model, the renormalization-group evolution of quenched random distributions has to be pursued. Initially, 5,000 nearest-neighbor Hamiltonians are created, with 10,000 randomly chosen magnetic field directions as described above. From this distribution,  $b^d$  nearest-neighbor Hamiltonians are randomly chosen, to effect the local Migdal-Kadanoff transformation and obtain a renormalized nearest-neighbor Hamiltonian. This is repeated 5,000 times and the renormalized distribution is obtained. Each nearest-neighbor Hamiltonian in the distribution is exponentiated and thus kept as a transfer matrix.[35, 38] To conserve, in this distribution, the  $(ij) \leftrightarrow (ji)$  and the random-field direction symmetries, each transfer matrix is replicated by its transpose and by the simultaneous cyclic permutations of the rows and columns. Of the resulting  $2q \times 5000$  matrices, 5,000 are randomly chosen. Thus, the distribution continues as 5,000  $q \times q$  matrices.

The flows of the distributions determine the phase diagram: Renormalization-group trajectories starting in the ferromagnetic phase flow to the strong-coupling sink of  $J_{ij} \rightarrow \infty, H_i = 0$ . Renormalization-group trajectories starting in the disordered phase flow to the decoupled sink of  $J_{ij}, H_i = 0$ . The boundaries between these flow basins are the phase boundaries.

### III. $d = 3$ DIMENSIONS AND ZERO-TEMPERATURE CRITICALITY SEGMENT

Our calculated phase diagrams for  $(q = 7, 10, 20, 50, 100, 150)$ -state random-field clock models in  $d = 3$  are in Fig. 2, occurring in the figure respectively from high field to low field. Disordered and ferromagnetic phases occur at high temperature-high field and low temperature-low field, respectively. The  $H/J$  values on the vertical axis are multiplied with  $q$ , originally for better graphical visibility, but eventually leading to a physical result, as seen here. Firstly, note that the ferromagnetic region under random fields recedes and disappears as  $q$  is increased. This result is even more evident, when we recall that the vertical axis values are amplified by a factor of  $q$  for better pictorial visibility. The ferromagnetic phase, in random field, disappearing as  $q \rightarrow \infty$  indicates that no ferromagnetic phase occurs in the random-field XY model at non-zero temperature in  $d = 3$ .

Secondly and quite interestingly, given our choice of vertical axis values, it revealed that the ordered phase extends at very low temperatures, for the high  $q$  to the

universal value of  $qH/J = 5.1$ . This is more visible in the left inset box of Fig. 2. Thus, at  $q \rightarrow \infty$ , a line segment of zero-temperature critical points occurs between  $qH/J = 0$  and  $qH/J = 5.1$ . Zero-temperature critical segments and multicritical points have been found before, under exact renormalization-group treatment, in the  $d = 1$  Blume-Emery-Griffiths model [39].

Thirdly, for high  $q$ , the zero-field ferromagnetic transition temperature saturates, as also seen in Ref.[38] and in detail in the right inset box in Fig. 2. Furthermore, when the vertical axis is scaled, not by  $q$ , but by  $q^2$ , a universal phase diagram emerges above low temperature for high  $q$ , as seen in Fig. 3.

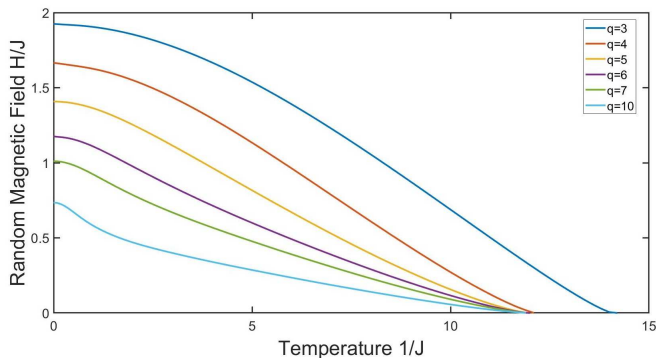


FIG. 4. Phase diagrams for  $(q = 3, 4, 5, 6, 7, 10)$ -state random-field clock models in  $d = 3.32$ , occurring in the figure respectively from high field to low field.

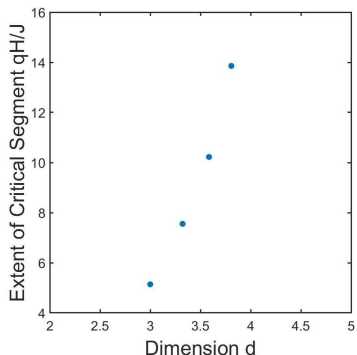


FIG. 5. The critical line segment, at zero temperature, is between  $qH/J = 0$  and the  $qH/J$  values shown in this figure for each dimension  $d$ . The values are consistent with a divergence as  $d = 4$  is approached.

#### IV. $d = 4$ DIMENSIONS AND THE LOWER-CRITICAL DIMENSION

The phase diagrams for  $(q = 3, 4, 5, 6, 7, 10)$ -state random-field clock models in  $d = 3.32$  are shown in Fig. 4. It is again seen that the ferromagnetic phase, under

random fields, recedes and disappears as  $q \rightarrow \infty$ . Thus,

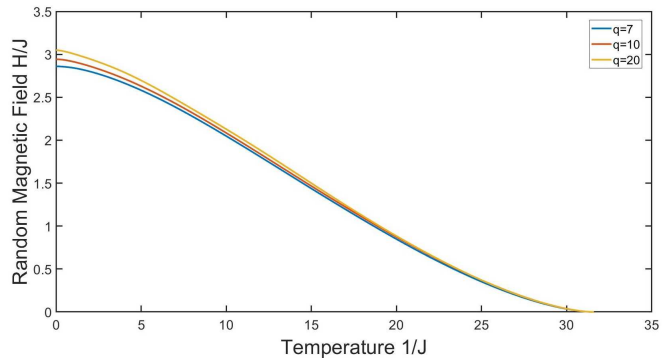


FIG. 6. Phase diagrams for  $(q = 7, 10, 20)$ -state random-field clock models in  $d = 4$ , occurring in the figure respectively from low field to high field.

no ferromagnetic phase occurs under random fields in the XY model in  $d = 3.32$ . However, our calculation again gives the zero-temperature critical segment, between  $qH/J = 0$  and  $qH/J = 7.6$  universally for all  $q$  in  $d = 3.32$ .

The same results are obtained for  $d = 3.58$  and  $3.81$ , with the zero-temperature critical segment expanding, reaching  $qH/J = 10.2$  and  $13.9$ , respectively.

A qualitatively different picture occurs in the phase diagrams for  $d = 4$ , seen in Fig. 5. Going from  $q = 7$  to  $q = 10$ , the ferromagnetic phase slightly expands in the random field, as opposed to drastically receding as in the lower dimensions. Going from  $q = 10$  to  $q = 20$ , a much larger  $q$  interval, the ferromagnetic phase even more slightly expands in the random field. Thus, the ferromagnetic phase occurs, under random fields, for  $q \rightarrow \infty$  and for the XY model in  $d = 4$ .

We thus see that the lower-critical dimension for the random-field XY model is between  $d = 3.81$  and  $d = 4$ , namely  $3.81 < d_c < 4$ .

#### V. CONCLUSION

In order to investigate the random-field XY model, we have studied the random-field  $q$ -state clock models for increasing  $q$ , for dimensions  $d = 3, 3.32, 3.58, 3.81, 4$ . We find that for the random-field XY model, the lower-critical dimension is between  $d = 3.81$  and  $d = 4$ , namely  $3.81 < d_c < 4$ . At  $d < d_c$ , we find a zero-temperature segment of criticality, stretching from zero to a value of  $qH/J$  that is  $q$ -independent for large  $q$  and that increases as  $d_c$  is approached.

#### ACKNOWLEDGMENTS

Support by the Academy of Sciences of Turkey (TÜBA) is gratefully acknowledged.

- 
- [1] D. P. Belanger, A. R. King, and V. Jaccarino, Random-field effects on critical behavior of diluted Ising antiferromagnets, *Phys. Rev. Lett.* **48**, 1050 (1982).
- [2] P.-Z. Wong and J. W. Cable, Hysteretic behavior of the diluted random-field Ising system  $Fe_{0.70}Mg_{0.30}Cl_2$ , *Phys. Rev. B* **28**, 5361 (1983).
- [3] A. N. Berker, Ordering under random fields: Renormalization-group arguments, *Phys. Rev. B* **29**, 5243 (1984).
- [4] H. Yoshizawa, R. A. Cowley, G. Shirane, R. J. Birgeneau, H. J. Guggenheim, and H. Ikeda, Random-field effects in two- and three-dimensional Ising antiferromagnets, *Phys. Rev. Lett.* **48**, 438 (1982).
- [5] M. S. Cao and J. Machta, Migdal-Kadanoff study of the random-field Ising model, *Phys. Rev. B* **48**, 3177 (1993).
- [6] A. Falicov, A. N. Berker, and S. R. McKay, Renormalization-group theory of the random-field Ising model in 3 dimensions, *Phys. Rev. B* **51**, 8266 (1995).
- [7] A. Aharony, Y. Imry, and S.-k. Ma, Lowering of dimensionality in phase transitions with random fields, *Phys. Rev. Lett.* **37**, 1364 (1976).
- [8] A. A. Migdal, Phase transitions in gauge and spin lattice systems, *Zh. Eksp. Teor. Fiz.* **69**, 1457 (1975) [*Sov. Phys. JETP* **42**, 743 (1976)].
- [9] L. P. Kadanoff, Notes on Migdal's recursion formulas, *Ann. Phys. (N.Y.)* **100**, 359 (1976).
- [10] A. N. Berker and S. Ostlund, Renormalisation-group calculations of finite systems: Order parameter and specific heat for epitaxial ordering, *J. Phys. C* **12**, 4961 (1979).
- [11] R. B. Griffiths and M. Kaufman, Spin systems on hierarchical lattices: Introduction and thermodynamic Limit, *Phys. Rev. B* **26**, 5022R (1982).
- [12] M. Kaufman and R. B. Griffiths, Spin systems on hierarchical lattices: 2. Some examples of soluble models, *Phys. Rev. B* **30**, 244 (1984).
- [13] K. Jiang, J. Qiao, and Y. Lan, Chaotic renormalization flow in the Potts model induced by long-range competition, *Phys. Rev. E* **103**, 062117 (2021).
- [14] G. Mograby, M. Derevyagin, G. V. Dunne, and A. Teplyaev, Spectra of perfect state transfer Hamiltonians on fractal-like graphs, *J. Phys. A* **54**, 125301 (2021).
- [15] I. Chio, R. K. W. Roeder, Chromatic zeros on hierarchical lattices and equidistribution on parameter space, *Annales de l'Institut Henri Poincaré D*, **8**, 491 (2021).
- [16] B. Steinhurst and A. Teplyaev, Spectral analysis on Barlow and Evans' projective limit fractals, *J. Spectr. Theory* **11**, 91 (2021).
- [17] A. V. Myshlyavtsev, M. D. Myshlyavtseva, and S. S. Aki- menko, Classical lattice models with single-node interactions on hierarchical lattices: The two-layer Ising model, *Physica A* **558**, 124919 (2020).
- [18] M. Derevyagin, G. V. Dunne, G. Mograby, and A. Teplyaev, Perfect quantum state transfer on diamond fractal graphs, quantum information processing, **19**, 328 (2020).
- [19] S.-C. Chang, R. K. W. Roeder, and R. Shrock, q-Plane zeros of the Potts partition function on diamond hierarchical graphs, *J. Math. Phys.* **61**, 073301 (2020).
- [20] C. Monthus, Real-space renormalization for disordered systems at the level of large deviations, *J. Stat. Mech. - Theory and Experiment*, 013301 (2020).
- [21] O. S. Sariyer, Two-dimensional quantum-spin-1/2 XXZ magnet in zero magnetic field: Global thermodynamics from renormalisation group theory, *Philos. Mag.* **99**, 1787 (2019).
- [22] J. V. José, L. P. Kadanoff, S. Kirkpatrick, and D. R. Nelson, Renormalization, vortices, and symmetry-breaking perturbations in 2-dimensional planar Model, *Phys. Rev. B* **16**, 1217 (1977).
- [23] A. N. Berker and D. R. Nelson, Superfluidity and phase separation in Helium films, *Phys. Rev. B* **19**, 2488 (1979).
- [24] E. Tunca and A. N. Berker, Renormalization-group theory of the Heisenberg model in d dimensions, arXiv:2202.06049 [cond-mat.stat-mech] (2022).
- [25] S. Franz, G. Parisi, and M.A. Virasoro, Interfaces and lower critical dimension in a spin-glass model, *J. Physique I* **4**, 1657 (1994).
- [26] C. Amoruso, E. Marinari, O. C. Martin, and A. Pagnani, Scalings of domain wall energies in two dimensional Ising spin glasses, *Phys. Rev. Lett.* **91**, 087201 (2003).
- [27] J.-P. Bouchaud, F. Krzakala, and O. C. Martin, Energy exponents and corrections to scaling in Ising spin glasses, *Phys. Rev. B* **68**, 224404 (2003).
- [28] S. Boettcher, Stiffness of the Edwards-Anderson model in all dimensions, *Phys. Rev. Lett.* **95**, 197205 (2005).
- [29] M. Demirtaş, A. Tuncer, and A. N. Berker, Lower-critical spin-glass dimension from 23 sequenced hierarchical models, *Phys. Rev. E* **92**, 022136 (2015).
- [30] A. Maiorano and G. Parisi, Support for the value 5/2 for the spin glass lower critical dimension at zero magnetic field, *Proc. Natl. Acad. Sci. USA* **115**, 5129 (2018).
- [31] B. Atalay and A. N. Berker, A lower lower-critical spin-glass dimension from quenched mixed-spatial-dimensional spin glasses, *Phys. Rev. E* **98**, 042125 (2018).
- [32] S. R. McKay, A. N. Berker, and S. Kirkpatrick, Spin-glass behavior in frustrated Ising models with chaotic renormalization-group trajectories, *Phys. Rev. Lett.* **48**, 767 (1982).
- [33] S. R. McKay, A. N. Berker, and S. Kirkpatrick, Amorphously packed, frustrated hierarchical models: Chaotic rescaling and spin-glass behavior, *J. Appl. Phys.* **53**, 7974 (1982).
- [34] A. N. Berker and S. R. McKay, Hierarchical models and chaotic spin glasses, *J. Stat. Phys.* **36**, 787 (1984).
- [35] S.E. Gürleyen and A.N. Berker, Asymmetric phase diagrams, algebraically ordered BKT phase, and peninsular Potts flow structure in long-range spin glasses, S.E. Gürleyen and A.N. Berker, *Phys. Rev. E* **105**, 024122 (2022).
- [36] T. Çağlar and A. N. Berker, Chiral Potts spin glass in  $d = 2$  and 3 dimensions, *Phys. Rev. E* **94**, 032121 (2016).
- [37] H. Y. Devre and A. N. Berker, First-order to second-order phase transition changeover and latent heats of q-state Potts models in  $d=2,3$  from a simple Migdal-Kadanoff adaptation, arXiv:2202.01528 [cond-mat.stat-mech] (2022).
- [38] E. C. Artun and A. N. Berker, Complete density calculations of q-state Potts and clock models: Reentrance of interface densities under symmetry breaking, *Phys. Rev. E* **102**, 062135 (2020).
- [39] S. Krinsky and D. Furman, Exact renormalization group exhibiting tricritical fixed point for a spin-one Ising model

in one dimension, Phys. Rev. B **11**, 2602 (1975).